Magnetization measurement of a possible high-temperature superconducting state in amorphous carbon doped with sulfur

Israel Felner[1] and Yakov Kopelevich[2]
[1]*Racah Institute of Physics, The Hebrew University, Jerusalem 91904, Israel*
[2]*Instituto de Física "Gleb Wataghin," Universidade Estadual de Campinas–UNICAMP, 13083-970 Campinas, SP, Brazil*
(Received 23 April 2009; revised manuscript received 8 June 2009; published 30 June 2009)

Magnetization $M(T,H)$ measurements performed on thoroughly characterized commercial amorphous carbon powder doped with sulfur (AC-S), revealed the occurrence of an inhomogeneous superconductivity (SC) below $T_c=38$ K. The constructed magnetic field-temperature (H-T) phase diagram resembles that of type-II superconductors. However, AC-S demonstrates a number of anomalies, such as: (1) a nonmonotonic behavior of the lower critical-field $H_{c1}(T)$; (2) a pronounced positive curvature of the apparent upper critical-field boundary $H_{c2}(T)$; and (3) a spontaneous ferromagneticlike magnetization M_0 coexisting with SC. Based on the analysis of experimental results we propose a nonstandard SC state in AC-S.

DOI: 10.1103/PhysRevB.79.233409 PACS number(s): 74.10.+v, 74.62.−c, 74.70.Wz, 74.81.−g

Recently, possible superconductivity (SC) in graphene (isolated graphitic layer) attracted considerable theoretical attention.[1–9] In many respects, this was motivated by the current interest of graphene itself,[10–12] and by observations of SC at elevated temperatures in related materials: doped fullerenes[13,14] graphite,[15–19] diamond,[20,21] and carbon nanotubes.[22,23] In particular, BCS type SC in graphene with a mean-field critical temperature T_c^{MF} up to ~150 K was calculated in Refs. 5 and 7, and T_c^{MF} well above the room temperature was predicted within the framework of the resonating valence bond (RVB) model,[1,8] proposed by Anderson[24] for high-T_c cuprates. From the experimental side, localized SC found for graphite-sulfur (G-S) composites[15–17] is perhaps the most suggestive realization of the theoretical expectations for the doping-induced SC in graphene.[1,2,4,8] Both d-wave[1,8] and p-wave[1,25,26] symmetries of the SC order parameter (OP) were predicted for graphene. The occurrence of p-wave SC in G-S is appealing, because it coexists with the ferromagnetism (FM),[27] and the interaction between SC and FM OPs has been experimentally demonstrated.[17] According to Ref. 25, the high-T_c p-wave SC emerges in a matrix of curved graphene layers with inserted pentagons and heptagons. If high-T_c p-wave SC exists in graphitic materials, this may have far-reaching consequences, due to the non-Abelian statistics of the vortices in p-wave SC, allowing for the quantum computation.[28] Hence, the research in this direction has a broad and an interdisciplinary interest. Amorphous carbon (AC) is a strongly disordered material consisting of a submicron curved graphene layers with a mixed interlayer stacking. AC also contains partially graphitized carbon fragments that possess both negative and positive curvatures, required for SC.[29] All these motivations triggered the present work.

This report is focused on experimental evidences for SC in sulfur-doped amorphous carbon (AC-S) occurring at $T<T_c=38$ K. The observed anomalous behavior of the lower and the apparent upper critical fields, as well as the coexistence of superconducting and ferromagneticlike states, all suggest an unconventional superconducting state in AC-S.

The pristine material is a 74-year-old commercial amorphous carbon powder manufactured by Fisher (C190-N) as decolorized carbon. The AC-S sample was obtained by mixing AC and sulfur (99.998%; Aldrich Chemical Co., Inc.) powders in a mass ratio $m_C:m_S=2:1$. The mixed powder was pressed and sealed in evacuated quartz tube and then heated at 250 °C for 24 h before cooling down to ambient temperature.

The samples were thoroughly characterized by means of x-ray diffraction (XRD), scanning electron microscopy (SEM), energy dispersive spectroscopy (EDS) JOEL JSM-7700 SEM, and ^{57}Fe Mossbauer spectroscopy. Trace element analysis was performed by means of the inductively coupled plasma mass spectrometer (ICPMS) (Perkin-Elmer ICP-OES model 3300) of acid extracts. $M(T,H)$ measurements up to $H=50$ kOe and $5\leq T\leq 300$ K were performed by using commercial (MPMS5 Quantum Design) superconducting quantum interference device (SQUID) magnetometer. Zero-field-cooled (ZFC) magnetization $M_{ZFC}(T,H)$ plots were measured via heating the samples after cooling at $H=0$. Prior to each ZFC measurement, the SQUID magnetometer was adjusted to compensate the remnant magnetic field of the SC solenoid. The field-cooled data $M_{FCC}(T,H)$ were taken under cooling in applied field.

The featureless XRD patterns obtained for both AC and AC-S samples are consistent with their amorphouslike structure. From SEM images, we found a broad distribution in the carbon "grain" size which ranges from ~10 nm to several microns. Spatially resolved elemental composition analysis on AC performed by EDS yields: Na [0.30(1) at. %], oxygen [2.44(1) at. %], and sulfur [0.21(1) at. %] as extra elements. The same analysis performed on AC-S sample showed: Na (0.35 at. %), oxygen (1.96 at. %), and sulfur (10.3 at. %). The mass ratio $m_C:m_S$ are 174 and 3 for AC and AC-S samples, respectively. Thus, the major difference between the AC and AC-S samples is the significant increase in the sulfur contents in AC-S. The trace element analysis of AC revealed impurities (ppm): V (2.05), Ni (2.77), Zn (7.09), Cu (11.1), Mn(133.1), Al (212.7), Fe (360.0), and Na (4625). It means that the total amount of magnetic impurities (Ni, Mn, and Fe) is about 486 ppm. Long-time (two weeks) room-temperature ^{57}Fe Mossbauer measurements, performed on AC sample, revealed a broad magnetic spectrum with two sextets, with an estimated Fe concentration of $\sim 350\pm 50$ ppm. A least-squares fit provides evidence that the magnetic sextets are related to magnetite (Fe_3O_4). From

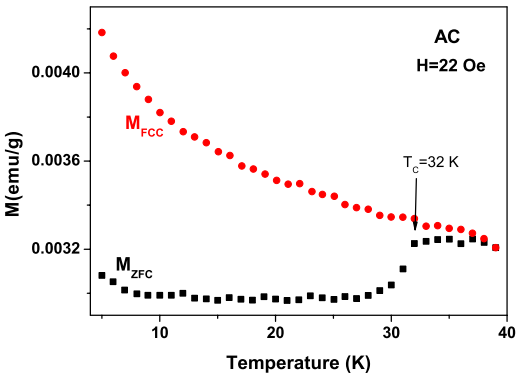

FIG. 1. (Color online) $M_{ZFC}(T)$ and $M_{FCC}(T)$ measured for pristine AC at $H=22$ Oe.

$M(H)$ measurements of AC, we deduced a spontaneous FM magnetization of $M_m \approx 0.033$ emu/g. This value corresponds to 350 ppm of Fe_3O_4 ($M_S=94.5$ emu/g) and is in a perfect agreement with that obtained from Mossbauer measurements.

Figure 1 shows $M_{ZFC}(T,H)$ and $M_{FCC}(T,H)$ curves measured for the pristine AC sample at $H=22$ Oe. Figure 2(a) presents $M_{ZFC}(T,H)$ and $M_{FCC}(T,H)$ of AC-S, measured at $H=50$ Oe up to 275 K. The low-temperature range of Fig. 2(a) as well as the remnant magnetization M_{REM} $(T,H=0)$, recorded after the FCC process when the field was switched off at $T=5$ K, are exhibited in Fig. 2(b). Here, the irrelevant temperature-independent background magnetization $M_m=0.037$ emu/g measured for this sample was subtracted from all three branches. As Fig. 2(b) demonstrates, below $T_c \sim 38$ K, the magnetization is strongly irreversible and $M_{FCC}(T) > M_{ZFC}(T)$. Both $M_{ZFC}(T)$ and $M_{REM}(T)$ show a pronounced steplike feature at $T_c \sim 38$ K. Importantly, $M_{FCC}(T)$ also demonstrates a clear drop (though, smaller in amplitude) below T_c. It appears, that below T_c $M_{ZFC}(T)$ is negative (diamagnetic), as expected for SC, where the diamagnetism originates from screening supercurrents, and the drop of $M_{FCC}(T)$ is associated with the magnetic-flux expulsion due to Meissner effect (ME). Then, it is reasonable to relate $M_{REM}(T)$ to the trapped magnetic flux (vortices). The estimated shielding fraction deduced from $M_{ZFC}(T)$ and the Meissner fraction (MF) are $\sim 0.15\%$ and $\sim 0.02\%$, respectively. Since no corrections for carbon magnetism (see below) and for the flux trapping effects were made, the ME provides only the lower limit for the SC volume fraction. Nevertheless, the smallness of both shielding and MF values suggests an inhomogeneous SC state in AC-S. The data presented in Fig. 1 suggest also a possible SC state with $T_c=32$ K in AC with a shielding fraction of $\sim 0.03\%$, a value which is five times smaller than that obtained for AC-S. The much smaller shielding fraction in AC would explain the invisibility of the Meissner signal in $M_{FCC}(T)$ in Fig. 1. Since the AC and AC-S samples differ only in their sulfur contents, it is reasonable to assume that the SC state observed for AC (Fig. 1) is triggered by sulfur. Adding sulfur to AC (Fig. 2), both T_c and the SC fraction are enhanced.

Figures 3(a) and 3(b) show the normalized ZFC magnetization $M_{ZFC}(T)/M_{ZFC}(40\ \text{K})$ measured for various fields. As Fig. 3(b) exemplifies, $T_c(H)$ at lower fields can be well

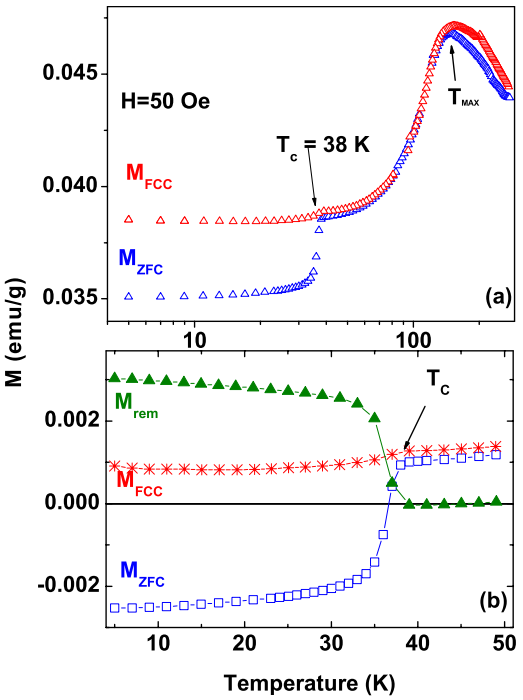

FIG. 2. (Color online) (a) $M_{ZFC}(T)$ and $M_{FCC}(T)$ of AC-S measured at $H=50$ Oe up to 275 K; $T_c=38$ K and $T_{max}=150$ K are noted by arrows. (b) A detailed view of $M_{ZFC}(T)$ and $M_{FCC}(T)$ curves shown in (a) as well as M_{REM} $(T,H=0)$. The background magnetization $M_m=0.037$ emu/g due to Fe_3O_4 is subtracted from all three branches.

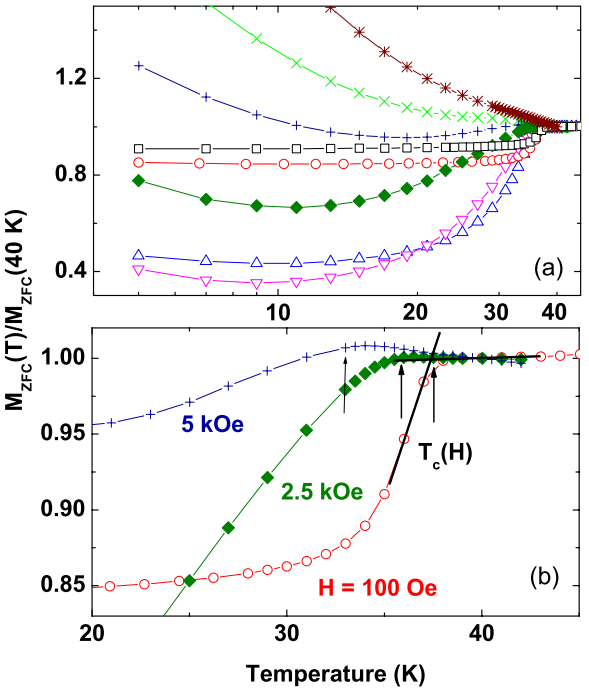

FIG. 3. (Color online) (a) (AC-S) Normalized $M_{ZFC}(T)$ plots, measured for $H=50$ Oe (□), 100 Oe (○), 500 Oe (△), 1 kOe (▽), 2.5 kOe (◇), 5 kOe (+), 10 kOe (x), and 25 kOe (*); (b) the same as in (a) for three measuring fields; arrows indicate $T_c(H)$ as defined for $H=100$ Oe.

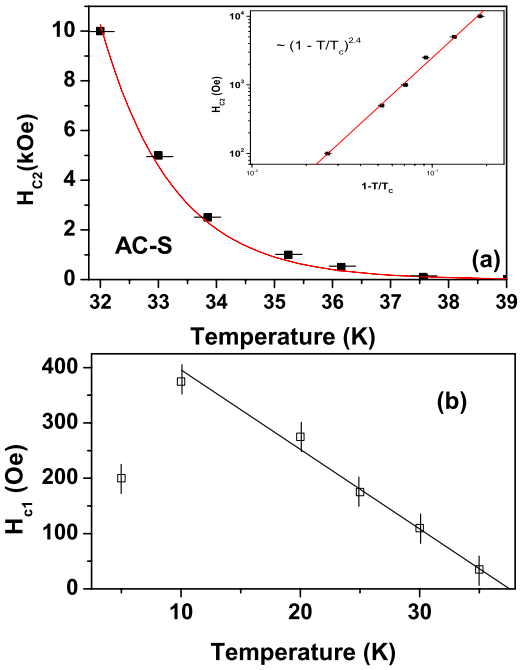

FIG. 4. (Color online) (a) (AC-S) The apparent upper critical-field boundary $H_{c2}(T)$. The solid line corresponds to Eq. (1). The double-logarithmic plot of $H_{c2}(T)$ vs $1-T/T_c$ is presented in the inset. (b) Lower critical-field $H_{c1}(T)$ obtained as indicated in Fig. 5 (upper inset); the straight line is the linear fit: $H_{c1}(T)=H_{c1}(0)$ $(1-T/T_c)$ with $H_{c1}(0)=550$ Oe and $T_c=38$ K.

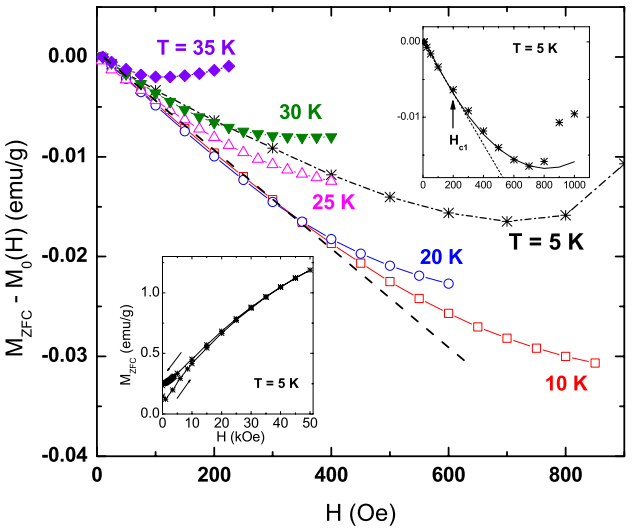

FIG. 5. (Color online) (AC-S) Low-field portions of various $M_{ZFC}(H)$ isotherms after subtraction of the spontaneous ZFC magnetization $M_0(H)$ (see Fig. 6 and the text). The upper inset exemplifies the validity of Eq. (2) that fits $M_{ZFC}(H)$ for $T=5$ K (solid line) with $M_0=0.04$ emu/g, $H_{c1}=200$ Oe, and $c=10^{-3}$. The dotted straight line is $M_{ZFC}(H)=-\chi_d B$, $|\chi_d|=3.4\times10^{-5}$ emu/g Oe. The lower inset shows $M_{ZFC}(H)$ hysteresis loop measured at $T=5$ K up to $H=50$ kOe.

defined. For $H=25$ kOe Fig. 3(a), the SC-like transition is suppressed (masked) and the (reversible) magnetization demonstrates a paramagnetic (PM) behavior. The phase boundary $T_c(H)\equiv H_{c2}(T)$ deduced from Fig. 3, which presumably separates the SC and normal states, is shown in Fig. 4(a). The PM at high applied fields limited the available for analysis experimental points to $t=T/T_c\geq0.8$. The obtained data points can be best fitted by the power law

$$H_{c2}(T)=H_{c2}(0)(1-T/T_c)^{\alpha}, \tag{1}$$

where $\alpha=2.4\pm0.2$, $H_{c2}(0)=6.5\cdot10^5$ Oe, and $T_c=38$ K.

The low-field portions of various $M_{ZFC}(H)$ isotherms measured for AC-S are presented in Fig. 5. For $H<H_{c1}(T)$, the $M_{ZFC}(T,H)$ linearly decrease with H, (see the main panel and the upper inset in Fig. 5) as expected for SC in the Meissner state. $M_{ZFC}(H)=M_0-\chi_d(T)H$, where $\chi_d(T)$ is the absolute value of the diamagnetic susceptibility, and $M_0\geq0$ is the spontaneous magnetization whose values depend on a thermomagnetic sample history (see below). The estimated shielding fraction extracted from χ_d is 0.13%. Noting, that M_0 does not alter $\chi_d(T)$. Unexpectedly, $|\chi_d(5\ \text{K})|$ is smaller than that measured at $T=10-25$ K. It should be also emphasized that the M_0 $(H=0,\ T=5\ \text{K})\approx0.24$ emu/g is ~7 times bigger than $M_m\approx0.037$ emu/g attributed to Fe_3O_4, i.e., the M_0 is essentially related to the AC-S matrix. $M_{ZFC}(H)$ deviates from the linearity for $H\geq H_{c1}(T)$. The $H_{c1}(T)$ is plotted in Fig. 4(b), where the straight line is obtained from the equation $H_{c1}(T)=H_{c1}(0)(1-T/T_c)$ with $H_{c1}(0)=550$ Oe. Note, the anomalous drop of H_{c1} at $T=5$ K. The lower inset in Fig. 5 presents the $M_{ZFC}(H)$ hysteresis loop measured at $T=5$ K up to $H=50$ kOe. The PM behavior is evident from the reversible nonsaturating high-field portion of the $M(H)$, giving the PM susceptibility $\chi_p\approx10^{-5}$ emu/g Oe, that fits well to the known χ_p values for disordered carbon materials (see, e.g., Ref. 30).

Figure 6 sheds light on the origin of M_0. The AC-S sample was first cooled from $T=300$ K to $T=5$ K at $H=0$. Then, $M_{ZFC}(T)$ at 50 Oe was measured (step 1). Above T_C (at $T=40-43$ K) the field was switched off and M_{REM} was recorded (step 2). Next, the sample was cooled down to 5 K, and M_0 was measured (step 3). After that, a higher field was applied and the same procedure was repeated. The $M_{ZFC}(T,H)$ curves obtained at various fields are depicted in Figs. 6(a)–6(c). As can be seen, $M_{REM}(T>T_c)=M_0(T=5\ \text{K})$. It also appears that M_{REM} $(M_0)\sim H^{\nu}$ with $\nu=0.4$. The occurrence of M_{REM}, and its increase with the field are characteristic features of FM. As stated above, it is reasonable to relate M_0 with the FM state associated with the carbon matrix. However, Fig. 2(a) does not reveal any signature for a FM transition in the entire temperature interval up to 275 K. On the contrary, for $T<T_{max}\approx150$ K, both $M_{ZFC}(T)$ and $M_{FCC}(T)$ decrease with the temperature decreasing. Such magnetic behavior is consistent with the occurrence of antiferromagnetic correlations competing with the FM order. In addition, $M_0\approx0.24$ emu/g obtained from $M(H)$ at $T=5$ K (Fig. 5, lower inset) agrees well with $M_0(H)\sim H^{0.4}$ dependence, indicating that $M_0(M_{REM})$ mainly originates from the FM state and not from trapped SC vortices. Heating the sample to room temperature totally suppresses M_{REM}.

Whereas it is too premature to speculate on the anomalous behavior of the apparent upper and lower critical fields, as well as on the origin of carbon-related magnetism, a brief comment should be instructive. In conventional SC, near T_c,

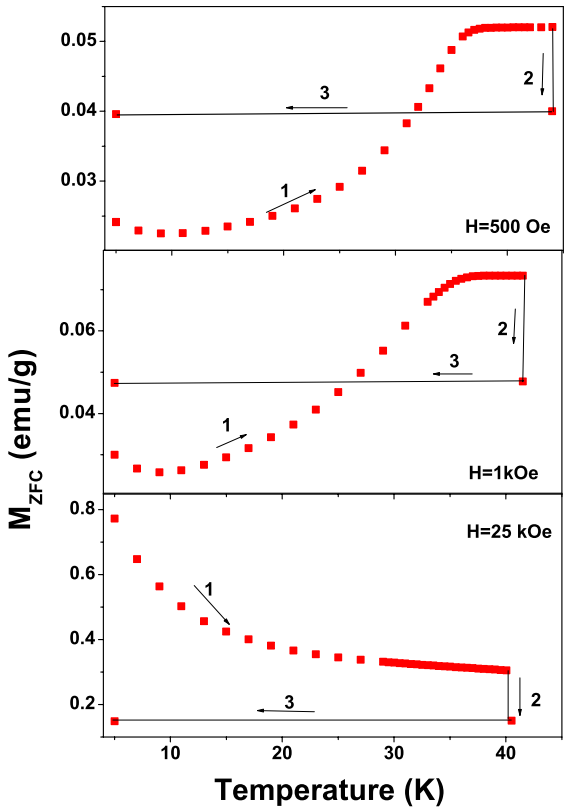

FIG. 6. (Color online) (AC-S) (a), (b), and (c) $M_{ZFC}(T,H)$ at various applied fields, illustrating the appearance of $M_0(H)$. All the measurements were made in the sequence $1\rightarrow 2\rightarrow 3$ as indicated in the figures.

$H_{c2}(T)\sim(1-T/T_c)$ for bulk, and $H_{c2}(T)\sim(1-T/T_c)^{1/2}$ for granular SC.[31] Therefore, the positive curvature in $H_{c2}(T)$ [Fig. 4(a)] may imply either an unconventional character of SC (Ref. 32) or the vortex lattice melting phase transition.[33] The high exponent obtained $\alpha=2.4\pm0.2$ is expected for the melting of Skyrmion flux (SF) lattice in p-wave SC,[34] where Skyrmion is a coreless vortexlike structure carrying two or more flux quanta $\Phi_0=h/2e$. In addition, close to $H_{c1}(T)$, all $M_{ZFC}(H)$ isotherms (Fig. 5) can be best fitted by the equation

$$M_{ZFC}(H) = M_0 - \chi_d H + c(H/H_{c1} - 1)^2, \qquad (2)$$

expected for the SF lattice state.[35] Hence, the occurrence of p-wave superconductivity in AC-S cannot be excluded.

In conclusion, we observed clear evidences for inhomogeneous SC in sulfur-doped amorphous carbon at $T_c=38$ K. The obtained results are consistent with the p-wave symmetry of the superconducting order parameter. The present work triggers other important questions such as: (i) whether SC in AC-S and in G-S composites is of the same origin. Besides the fundamental question on the nature of (inhomogeneous) FM in graphitic materials,[27] also supported by the present work, (ii) what is the interrelation between FM and SC states? Most importantly, a systematic experimental work, aiming to increase the reproducibility as well as the SC volume fraction in doped AC, is needed.

This work was supported by the Klachky Foundation for Superconductivity, FAPESP and CNPq. Y.K. also gratefully acknowledges the Lady Davis Foundation. We thank I. Nowik for Mossbauer measurements, E. B. Sonin for useful discussions, and Yuval Simons for his assistance.

[1] A. M. Black-Schaffer and S. Doniach, Phys. Rev. B **75**, 134512 (2007).
[2] B. Uchoa and A. H. Castro Neto, Phys. Rev. Lett. **98**, 146801 (2007).
[3] C. Honerkamp, Phys. Rev. Lett. **100**, 146404 (2008).
[4] N. B. Kopnin and E. B. Sonin, Phys. Rev. Lett. **100**, 246808 (2008).
[5] K.-I. Sasaki *et al.*, J. Phys. Soc. Jpn. **76**, 033702 (2007).
[6] P. Ghaemi and F. Wilczek, arXiv:0709.2626 (unpublished).
[7] D. V. Khveshchenko, J. Phys.: Condens. Matter **21**, 075303 (2009).
[8] S. Pathak, V. B. Shenoy, and G. Baskaran, arXiv:0809.0244 (unpublished).
[9] P. Panigrahi, V. Vyas, and T. Shreecharan, arXiv:0901.1034 (unpublished).
[10] A. K. Geim and A. H. MacDonald, Phys. Today **60** (8), 35 (2007).
[11] Y. Kopelevich and P. Esquinazi, Adv. Mater. **19**, 4559 (2007).
[12] A. H. Castro Neto *et al.*, Rev. Mod. Phys. **81**, 109 (2009).
[13] A. F. Hebard *et al.*, Nature (London) **350**, 600 (1991).
[14] K. Tanigaki *et al.*, Nature (London) **352**, 222 (1991).
[15] R. R. da Silva, J. H. S. Torres, and Y. Kopelevich, Phys. Rev. Lett. **87**, 147001 (2001).
[16] Y. Hai-Peng *et al.*, Chin. Phys. Lett. **18**, 1648 (2001).
[17] S. Moehlecke, Y. Kopelevich, and M. B. Maple, Phys. Rev. B **69**, 134519 (2004).
[18] T. E. Weller *et al.*, Nat. Phys. **1**, 39 (2005).
[19] N. Emery *et al.*, Phys. Rev. Lett. **95**, 087003 (2005).
[20] E. A. Ekimov *et al.*, Nature (London) **428**, 542 (2004).
[21] M. Ortolani *et al.*, Phys. Rev. Lett. **97**, 097002 (2006).
[22] Z. K. Tang *et al.*, Science **292**, 2462 (2001).
[23] I. Takesue *et al.*, Phys. Rev. Lett. **96**, 057001 (2006).
[24] P. W. Anderson, Science **235**, 1196 (1987).
[25] J. Gonzalez, F. Guinea, and M. A. H. Vozmediano, Phys. Rev. B **63**, 134421 (2001).
[26] K. V. Samokhin, Phys. Rev. B **66**, 212509 (2002).
[27] Y. Kopelevich and P. Esquinazi, J. Low Temp. Phys. **146**, 629 (2007).
[28] D. A. Ivanov, Phys. Rev. Lett. **86**, 268 (2001).
[29] P. J. F. Harris, A. Burian, and S. Duber, Philos. Mag. Lett. **80**, 381 (2000).
[30] Y. Shibayama, H. Sato, T. Enoki, and M. Endo, Phys. Rev. Lett. **84**, 1744 (2000).
[31] G. Deutscher, O. Entin-Wohlman, and Y. Shapira, Phys. Rev. B **22**, 4264 (1980).
[32] V. N. Zavaritsky, V. V. Kabanov, and A. S. Alexandrov, Europhys. Lett. **60**, 127 (2002).
[33] G. Blatter and B. I. Ivlev, Phys. Rev. B **50**, 10272 (1994).
[34] Q. Li, J. Toner, and D. Belitz, Phys. Rev. Lett. **98**, 187002 (2007).
[35] A. Knigavko and B. Rosenstein, Phys. Rev. Lett. **82**, 1261 (1999).